16 OROGRAPHIC EFFECTS ON TRACK DEFLECTION OF IDEALIZED TROPICAL CYCLONES

Shu-Hua Chen[1,*], Yuh-Lang Lin[2,3], and Liping Liu[4]
Department of Land, Air, and Water Resources[1]
University of California, Davis, California[1]
Department of Physics[2]
Department of Energy and Environmental Systems[3]
Department of Mathematics[4]
North Carolina A&T State University, Greensboro, North Carolina

1. INTRODUCTION

The interactions between tropical cyclones (TCs) and mesoscale mountain ranges have been studied extensively in the past 2-3 decades. Examples are like typhoons interacting with Taiwan's Central Mountain Range and the Cordillera Central of northern Luzon in Philippines (e.g., Chang 1982; Yeh and Elsberry 1993a,b; Lin et al. 2005; see Ch. 5 of Lin 2007 for a brief review) and hurricanes interacting with the southern-central Appalachians (Harville 2009), the Cordillera Central of Hispaniola (Bender et al. 1987), and the Sierra Madre of Mexico (Zehnder 1993; Zehnder and Reeder 1997). However, some fundamental dynamics of TCs over mesoscale mountain ranges are still not well understood. This study uses idealized simulations to improve our understanding of dynamical and physical processes influenced by orography, similar to those of Lin et al. (1999, 2005) and Lin and Savage (2011) but with the inclusion of moisture and planetary boundary layer.

2. THE NUMERICAL MODEL AND EXPERIMENT DESIGN

The model used for this study is the Advanced Research WRF (ARW) model version 3.4.1 (Skamarock et al. 2008). ARW model is a fully compressible, three-dimensional, nonhydrostatic model using terrain-following vertical coordinates. The governing equations for ARW are written in flux-form with conserved mass and dry entropy. In this study, the Runge-Kutta third-order time scheme is employed, and the fifth- and third-order advection schemes are used for the horizontal and vertical directions, respectively.

For numerical simulations, we utilize a single domain with a horizontal resolution of 15 km. The grid points are 433 x 433 in the x-y directions. In the vertical direction, the grids are stretched from the surface to the model top (~20 km) with a total of 41 levels. An elongated mountain range, which is oriented in the north-south direction, is placed in the domain. The shape of the mountain is defined as the following:

$$h(x,y)=\frac{h_o}{[1+(x-x_o)^2/a^2]^{3/2}} \quad for\ |y-y_o|\le b/2 \qquad (1a)$$

$$h(x,y)=\frac{h_o}{[1+(x-x_o)^2/a^2+(y-y_o)^2/b^2]^{3/2}} \qquad (1b)$$
$$for\ |y-y_o|>b/2$$

where h_o is the height of the mountain range, a =100 km, b =800 km, and (x_o, y_o) is the center position of the mountain locating at (180, 217). All cases in this study have the mountain width of $L_x=4a$ in the east-west and the length of $L_y=b+4a$ in the north-south direction.

Table 1: Numerical experiment design for Bogus TC over mountains.

Case	h (km)	Initial V_{max} (m/s)	Final V_{max} (m/s)	U/Nh	V_{max} /Nh	Characteristics
U5-F	0	21	55			No mountain, *f*-plane at 20°N
U5-B	0	21	55			No mountain, β-plane at 20°N
M1km	1	21	55	0.5	5.5	Control case
M2km	2	21	55	0.25	2.75	2 km high mountain
M1SV	1	15	25	0.5	2.5	Weaker initial vortex
M2NH	2	21	55	0.25	2.75	No latent heating
M2NHP	2	21	55	0.25	2.75	No latent heating; No PBL

*U=-5 m/s and N is assumed to be 0.01 s^{-1}.

Table 1 shows the seven numerical experiments that are conducted in this study. In these simulations, initial conditions are created by an offline code that was developed by Nolan (2011, 2013). The created initial vortex and environment conditions using a point-downscaling approach are then interpolated into WRF ARW. In the offline code, a bogus vortex is specified by the maximum tangential wind (V_{max}), which is given in Table 1, and the radius of V_{max}, which is 100 km.

Different numerical experiments are designed to investigate the impact of different factors on TC track deflection, such as the mountain height, the intensity of the initial bogus vortex (V_{max}), and the deactivation of specific physical processes. A periodic boundary condition is applied to the lateral boundaries. A 5-km sponge layer is added to the top of the physical domain to damp reflected gravity waves from the model top. The

**Corresponding author address*: Dr. Shu-Hua Chen, Dept. of Land, Air, and Water Resources, University of California, One Shields Avenue, Davis, 95616.
E-mail: shachen@ucdavis.edu

WRF model integrates for 10 days with a time step of 45 s.

Unless mentioned, the physics parameterization schemes for all experiments are: Kain-Fritsch cumulus parameterization scheme (Kain and Fritsch, 1993; Kain 2004), Purdue-Lin microphysics (Lin et al., 1983, Rutledge and Hobbs 1984, Chen and Sun 2002), YSU planetary boundary layer (PBL) parameterization scheme (Hong and Pan 1996), Monin-Obukov surface layer scheme (Monin and Obukhov, 1954), unified NOAH land-surface processes scheme (Tewari et al. 2004), and second-order diffusion on coordinate surfaces. The longwave and shortwave radiation parameterization schemes are excluded and an aqua planet is assumed. Details of the above schemes and their relevant references can be found in the ARW user manual (Skamarock et al. 2008).

3. OROGRAPHIC EFFECTS ON TC TRACK

3.1 Movement of TC in a uniform flow on an f- or a β-plane

Before investigating the orographic effects on TC tracks, the numerical simulations of bogus TCs embedded in a -5 m s^{-1} uniform flow on an *f*- or a β-plane without a mountain (i.e., U5-F vs. U5-B) are verified. On an *f*-plane, the simulated TC deflects to the south slightly (Fig. 3.1a), while on a β-plane, the simulated TC moves toward northwest (Fig. 3.1b). This is consistent with previous studies (e.g., Holland 1983; Chan and Williams 1987; Fiorino and Elsberry 1989) and explained by the advection of the ventilation flow between two beta gyres induced by the planetary vorticity advection (Holland 1983, Chan and Williams 1987) and by nonlinear asymmetric flow (Fiorino and Elsberry 1989) (see e.g., Figs. 9.28 and 9.29 and related review in Lin 2007).

3.2 Case M1km (vortex over 1-km high mountain)

For an idealized bogus vortex embedded in a -5 m s^{-1} easterly flow over a 1-km high mountain (i.e., the control case), the bogus vortex develops into a TC with V_{max}=55 m s^{-1}. The basic-flow Froude number (U/Nh) is about 0.5 and the vortex Froude number (V_{max}/Nh) is about 5.5. The TC is deflected to the south over the eastern slope and then resumes its westward movement over the western slope (i.e., the lee side of the mountain) (Fig. 3.2a). Note that this case is similar to that in the moderate blocking regime as classified in Lin et al. (2005 JAS – L05), except the vortex is moving southward due to stronger blocking with longer mountain range.

When the basic flow crosses over a mesoscale mountain range on an *f*-plane, the depth of air-column becomes shallower, compared to it far upstream, and induces a high (anticyclonic) pressure anomaly that is symmetric across the top of the range through vorticity stretching effect. The southward deflection over the upslope of the mountain is also enhanced by the interaction of the mountain and the outer circulation of the cyclone vortex through vorticity stretching, based on vorticity budget analysis (see Liu et al. 2014). Once the vortex crosses the mountain, it resumes its easterly movement.

The rainfall is accumulated along the TC track, as produced by the convection associated with eyewall and rainbands. When the TC is traveling on the upslope side of the mountain, rainfall is enhanced by the lifting of the mountain (Fig. 3.3). Light rainfall at the windward slope is also produced due to the mean flow impinging the mountain and producing upward motions and clouds (Fig. 3a).

The vertical structure of the TC becomes asymmetric during and after the passage over the mountain and the downstream flank of the eyewall is significantly weakened by the mountain (Figs. 3.3 and 3.4).

3.3 Case M2km (vortex over 2-km high mountain)

When the mountain height increases to 2 km, the orographic blocking is much stronger than that over the 1-km high mountain. The basic-flow Froude number (U/Nh) and the vortex Froude number (V_{max}/Nh) are reduced to 0.25 and 2.75, respectively. Similar to the control case (1-km high mountain, it is deflected to the south over the eastern slope, but much more significantly, and then resume its westward movement over the western slope and lee of the mountain (Fig. 3.5a). The storm is significantly weakened after passing the mountain (Fig. 3.5b-d). Similar to the 1-km high mountain (control) case, this case belongs to the moderate blocking case since the track is continuous.

3.4 Case M1SV (weaker vortex over a 1-km high mountain)

In order to test the track control parameters, we simulate a case identical to the control case (Case M1km) but with the initial strength of the bogus vortex reduced to 15 m s^{-1}, instead of 21 m s^{-1}. The initial vortex develops to a full strength TC with V_{max} = 25 m s^{-1}, which gives a vortex Froude number (V_{max}/Nh) of about 2.5. Taking the accumulated rain as a proxy of the TC track (Fig. 3.6), it is continuous. This is consistent with the threshold of V_{max}/Nh > 1.5 for a continuous TC track, as proposed by L05. To test the theory, we are in the process of testing cases with even smaller V_{max}/Nh.

4. MOISTURE AND PBL EFFECTS

The latent heat released by the TC impacts on the TC structure and track significantly as demonstrated by Fig. 4.1. When the cyclone comes closer to the mountain, e.g. t = 108 h (Fig. 4.1b), it becomes weaker and is deflected to the south by the mountain. The cyclone eventually is destroyed when it tries to climb over the mountain, e.g., t = 144 h (Fig. 4.1c). Note that at this time the 500-hPa circulation is located over the southern portion of the western slope of the mountain around (180, 160), and continues to move west-southwestward on the lee later on (not shown). A new cyclone then developed on the lee side (e.g., t = 180 h) at about (160, 205), thus makes the track appeared to be discontinuous. In fact, this new cyclone is developed

as a lee cyclone, instead of being spun up by the parent cyclone since the 500-hPa circulation is very weak and has moved to about the location of (150, 155). Thus, the surface bogus cyclone or vortex should be regarded as destroyed, instead of having discontinuous track. The maximum tangential wind speed is about 15 m s^{-1} upstream of the mountain, which gives V_{max}/Nh = 0.75. This falls to the strong blocking regime as proposed by L05.

In order to understand whether the PBL plays a role in this case, an experiment without latent heating and without PBL has been performed. Figure 4.2 shows the evolution of the relative vorticity field along the passage of the dry bogus vortex over a 2-km high mountain. It can be seen that the vortex is spun up to be stronger before arriving the foothill of the mountain (Fig. 4.2a, t = 72 h). The pair of cyclonic and anticyclonic lee vortices generated by the mountain is stronger, compare to those with PBL (Fig. 4.1). The cyclone has a maximum tangential velocity of about 20 m s^{-1}, which gives the vortex Froude number, V_{max}/Nh = 1. Similar to the case with PBL, the cyclone moves southward upstream of the mountain (Fig. 4.2b). At 144 h, two vorticity maxima can be found over the southwestern and northwestern slopes of the mountain and a band of high vorticity forms on the lee side of the mountain over the ocean (Fig. 4.2c). These high vorticity may be generated by vorticity stretching associated with the flow, either the basic flow or the circulation associated with the parent cyclone, over the mountain. The local vorticity maximum over the southwestern slope is co-located with the 500-hPa vortex (not shown) in vertical, which helps spin up to be a cyclone at a later time, such as at 180 h (Fig. 4.2d).

5. Summary

In this study, a number of idealized numerical experiments are performed using the Advanced Research Weather Research and Forecast (ARW) model to help understand the orographic effects on the track deflection and structure of tropical cyclones (TCs) in an aqua-planet. In these numerical experiments, TC is initialized by a bogus vortex in a conditionally unstable stratified airflow. For an idealized TC embedded in a -5 m s^{-1} easterly flow over a 1-km high mountain, the TC is deflected to the south upslope (eastern slope) and then to the north over the lee (western) slope while resuming its westward movement. The basic-flow and vortex Froude numbers are estimated to be U/ Nh = 0.5 and V_{max}/Nh = 5.5, respectively. Based on the findings of L05, this flow belongs to the moderately blocking regime but with stronger blocking due to much longer mountain range. For a 2-km high mountain, the TC track is similar to that of 1-km high mountain, but the southward deflection is much more pronounced. The accumulated rainfall is much stronger, extends farther along the mountain range, and produces much more rainfall at the upslope, compared with that over the 1-km high mountain. The estimated U/ Nh and V_{max}/Nh are 0.25 and 2.75 respectively, indicating that flow still belongs to the moderate blocking regime. Thus, the track is still continuous, consistent with L05's findings. Without latent heating, it is found that the dry vortex would be destroyed by the 2-km high mountain. Without both latent heating and planetary boundary layer forcing, the dry vortex is able to survive the orographic forcing, but its track becomes discontinuous in passing over a 2-km high mountain.

More cases, such as those of V_{max}/Nh < 1.5, with a β-plane, with no bogus vortex, and with land over the mountain area (island mountain cases), will be conducted. In addition, the mechanisms of track deflection with moisture will be explored by performing vorticity budget analysis.

ACKNOWLEDGMENTS: The help from Dr. David S. Nolan's on idealized WRF modeling with a bogus vortex is highly appreciated. This research is sponsored by the National Science Foundation Award AGS-1265783 and OCI-1126543. Dr. Chen is supported by the National Science Foundation Award-1015910.

6. REFERENCES

Bender, M. A., R. E. Tuleya, and Y. Kurihara, 1987: A numerical study of the effect of an island terrain on tropical cyclones. Mon. Wea. Rev., **115**, 130-155.

Chang, S. W.-J., 1982: The orographic effects induced by an island mountain range on propagating tropical cyclones. Mon. Wea. Rev., **110**, 1255-1270.

Chan, J. C. L., and R. T. Williams, 1987: Analytical and numerical studies of the beta-effect in tropical cyclone motion. Part I: zero mean flow. J. Atmos. Sci., **44**, 1257-1265.

Chen, S.-H., and W.-Y. Sun, 2002: A one-dimensional time-dependent cloud model, J. Meteor. Soc. Japan, **80**, 99-118.

Fiorino, M., and R. L. Elsberry, 1989: Some aspects of vortex structure related to tropical cyclone motion. J. Atmos. Sci., **46**, 975-990.

Harville, S. L., 2009: Effects of Appalachian topography on precipitation from landfalling hurricanes. MS thesis, North Carolina State University, 320pp. [Available from http://repository.lib.ncsu.edu/ir/handle/1840.16/2849]

Holland, G. J., 1983: Tropical cyclone motion: environmental interaction plus a beta-effect. J. Atmos. Sci., **40**, 328-342.

Hong, S.-Y., and H.-L. Pan, 1996: Non-local boundary layer vertical diffusion in Medium-Range Forecast model. Mon. Wea. Rev., **124**, 1215-1238.

Kain, J. S., 2004: The Kain-Fritsch convective parameterization: An update. J. Appl. Meteor., **43**, 170–181.

Kain, J. S., and Fritch, J. M., 1993: Convective parameterization for mesoscale models: The Kain-Fritsch scheme. *The representation of Cumulus Convection in Numerical Models, Meteor. Monogr.,* **24**, Amer. Meteor. Soc., 165-170.

Lin, Y.-L., and L. C. Savage III, 2011: Effects of landfall location and the approach angle of a cyclone vortex encountering a mesoscale mountain range. *J. Atmos. Sci.*, **68**, 2095-2106**.**

Lin, Y.-L., 2007: *Mesoscale Dynamics*. Cambridge Univ. Press, 630pp.

Lin, Y.-L., S.-Y. Chen, C. M. Hill, and C.-Y. Huang, 2005 (L05): Control parameters for tropical cyclones passing over mesoscale mountains, *J. Atmos. Sci.*, **62**, 1849-1866.

Lin, Y.-L., J. Han, D. W. Hamilton, and C.-Y. Huang, 1999: Orographic influence on a drifting cyclone. J. Atmos. Sci., **56**, 534-562.

Lin, Y.-L., Farley, R. D., and Orville, H. D., 1983: Bulk parameterization of the snow field in a cloud model. J. Clim. Appl. Meteor., **22**, 1065–1092. Paper No. 9.2, 16th Conf. on Mountain Meteorology, Amer. Meteor. Soc.

Monin A. S., and A. M. Obukhov, 1954: Basic laws of turbulent mixing in the surface layer of the atmosphere. Contrib. Geophys. Inst. Acad. Sci. USSR, **151**, 163–187 (in Russian).

Nolan, D. S., 2011: Evaluating environmental favorableness for tropical cyclone development with the methof of point-downscaling. J. Adv. Model. Earth Syst., **3**, Art. M08001, 28 pp.

Nolan, D. S., R. Atlas, K. T. Bhatia, and L. R. Bucci, 2013: Development and validation of a hurricane nature run using the joint OSSE nature run and the WRF model. J. Adv. Model Earth Syst., **5**, 1-24, doi:10.1002/jame.20031.

Rutledge, S.A. and P.V. Hobbs, 1984: The mesoscale and microscale structure and organization of clouds and precipitation in midlatitude cyclones. XII: A diagnostic modeling study of precipitation development in narrow cold-frontal rainbands. J. Atmos. Sci., **20**, 2949–2972.

Skamarock, W. C., J. B. Klemp, J. Dudhia, D. O. Gill, D. M. Barker, M. G. Duda, X.-Y. Huang, W. Wang, and J.G. Powers, 2008: A description of the advanced research WRF version 3. NCAR technical note, 113 pp. (also see http://www.mmm.ucar.edu/wrf/users/docs/arw_v3.pdf)

Tewari, M., F. Chen, W. Wang, J. Dudhia, M. A. LeMone, K. Mitchell, M. Ek, G. Gayno, J. Wegiel, and R. H. Cuenca, 2004: Implementation and verification of the unified NOAH land surface model in the WRF model. 20th Conf. Weather Analysis and Forecasting and 16th Conf. Numer. Wea. Pred., 11–15, Amer. Meteor. Soc.

Yeh, T.-C., and R. L. Elsberry, 1993a: Interaction of typhoons with the Taiwan topography. Part I: Upstream track deflection. Mon. Wea. Rev., **121**, 3193-3212.

Yeh, T.-C., and R. L. Elsberry, 1993b: Interaction of typhoons with the Taiwan topography. Part I: Continuous and discontinuous tracks across the island. Mon. Wea. Rev., **121**, 3213-3233.

Zehnder, J. A., 1993: The influence of large-scale topography on barotropic vortex motion. J. Atmos. Sci., **50**, 2519-2532.

Zehnder, J. A., and M. J. Reeder, 1997: A numerical study of barotropic vortex motion near a large-scale mountain range with application to the motion of tropical cyclones approaching the Sierra Madre. Meteor. Atmos. Phys., **64**, 1-19.

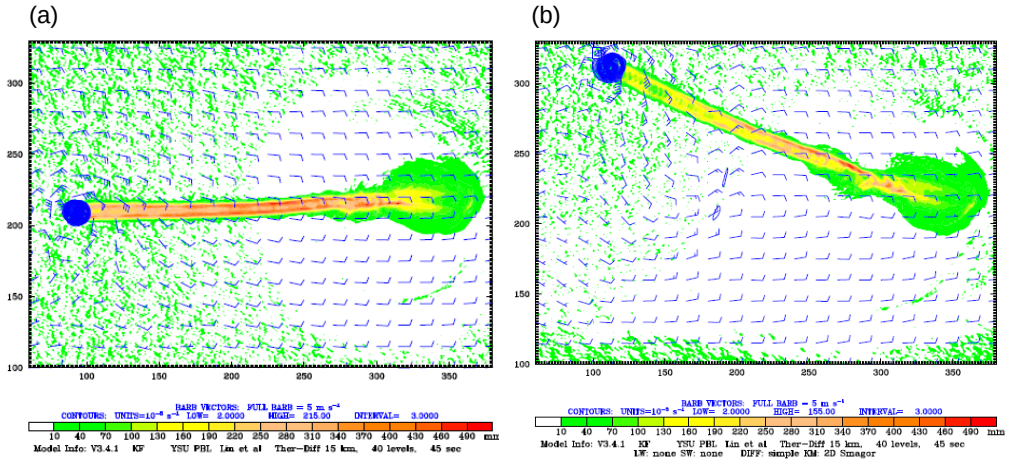

Fig. 3.1: The 500-hPa vector winds and vorticity fields, and accumulated rainfall at 240 h for (a) case U5-F (on an *f*-plane), and (b) case U5-B (on a β-plane). The *f*- or β-plane is centered at 20^{o}N. The β has a value of 9.27x10^{-12} m^{-1} s^{-1}.

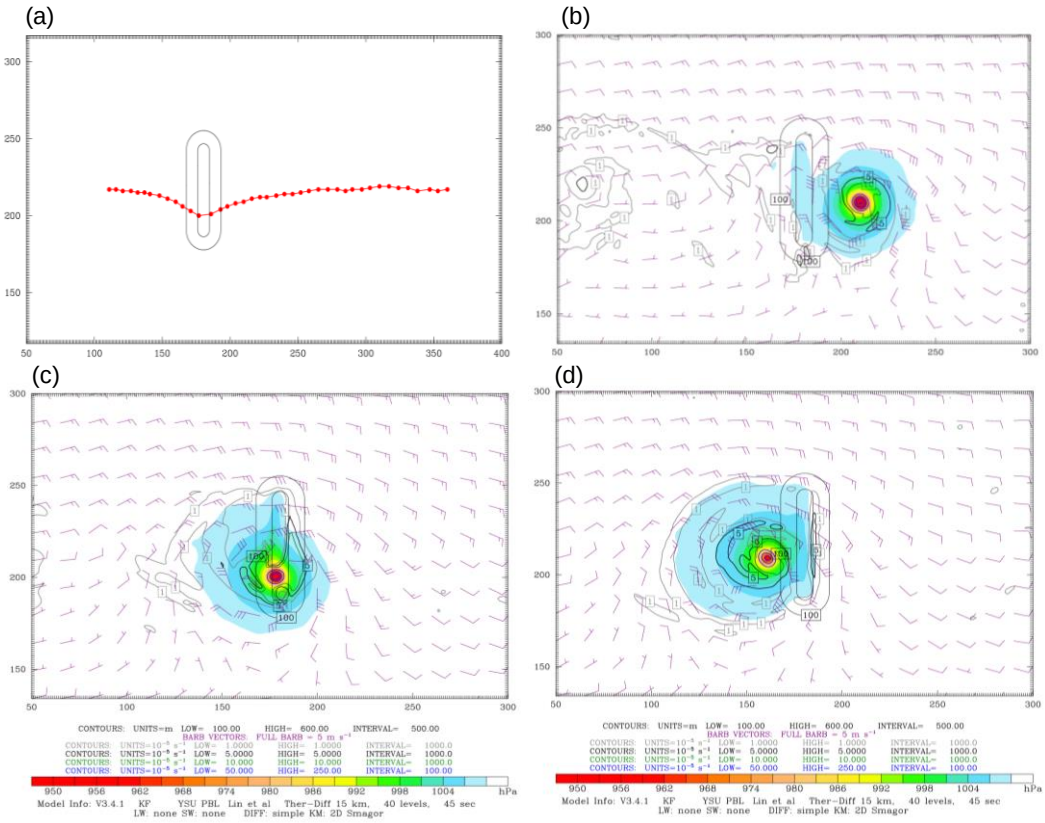

Fig. 3.2: [Case M1km] (a) TC track (based on minimum mean sea level pressure (SLP)). (b)-(d) 900-hPa wind vectors and vorticity (1x10^{-5} s^{-1}) and SLP (shaded; hPa) are shown at 138 h, 168 h and 186 h, respectively. The mountain height contours are 0.5 and 1 km.

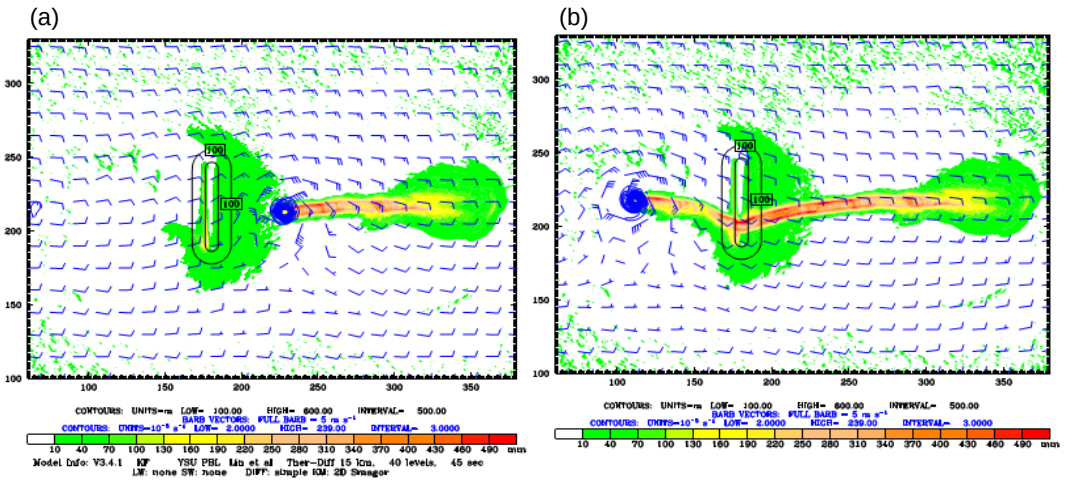

Fig. 3.3: [Case M1km] The 500-hPa wind vectors and vorticity fields (blue contours; $1x10^{-5}$ s^{-1}) and accumulated rainfall (shading; mm) at (a) 120 h and (b) 240 h.

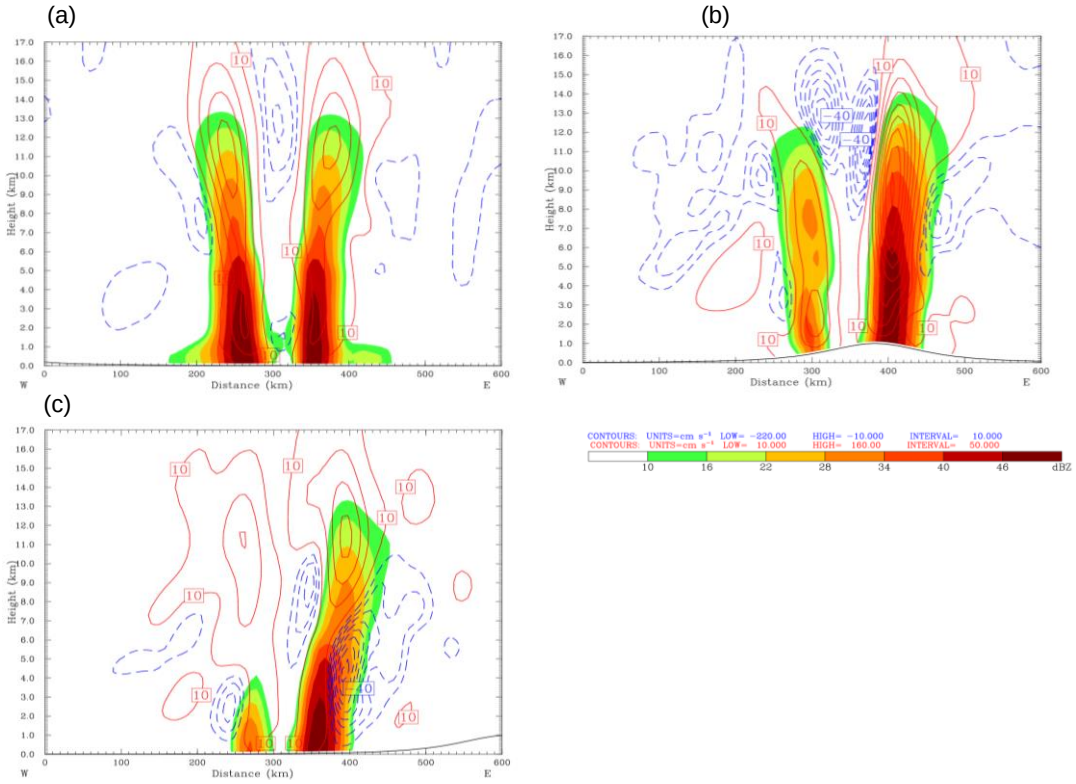

Fig. 3.4: [Case M1km] Vertical cross sections of w (contoured) and radar echoes (shaded): (a) 138 h, (b) 168 h, and (c) 186 h centered at y = 209, 200, and 209, respectively.

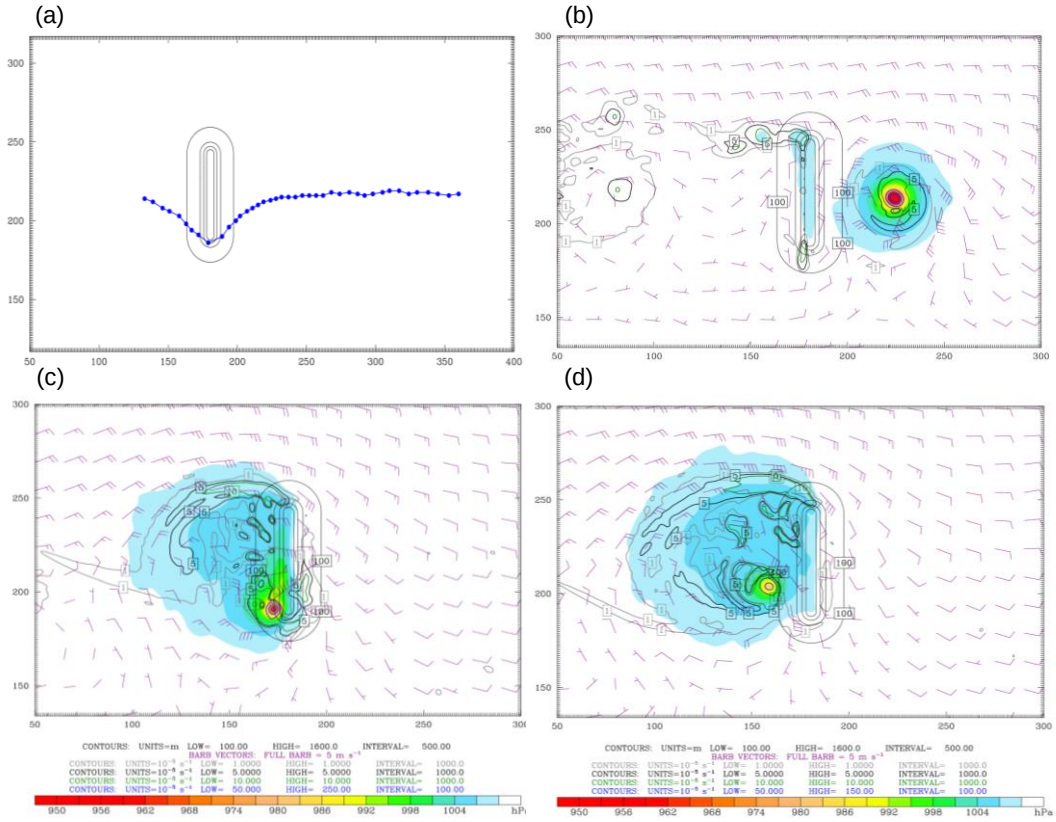

Fig. 3.5: [Case M2km] (a) TC track (based on MSLP). (b)-(d) 900-hPa wind vectors and vorticity ($1x10^{-5}$ s^{-1}) and SLP (shaded; hPa) are shown at 138h, 198h, and 216 h. The mountain height contours are 0.5 and 1 km. The easterly basic flow is 5 m s^{-1}.

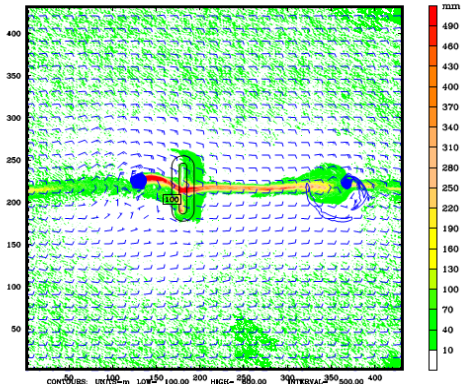

Fig. 3.6: Same as Fig. 3.3b but for a weaker TC passing over a 1-km high mountain (V_{max}/Nh=0.25).

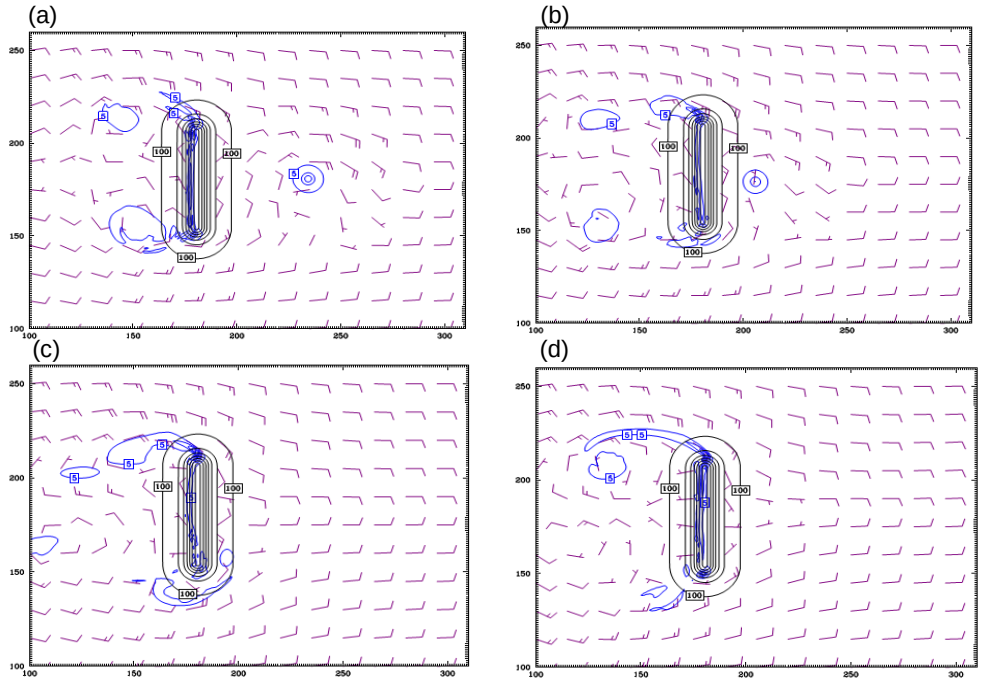

Fig. 4.1: [M2NH] The 900-hPa relative vorticity ($1x10^{-5}$ s^{-1}) and wind vectors simulated by a dry flow (no latent heating) with a bogus vortex over a 2-km high mountain at (a) 72 h, (b) 108 h, (c) 144 h, and (d) 180 h.

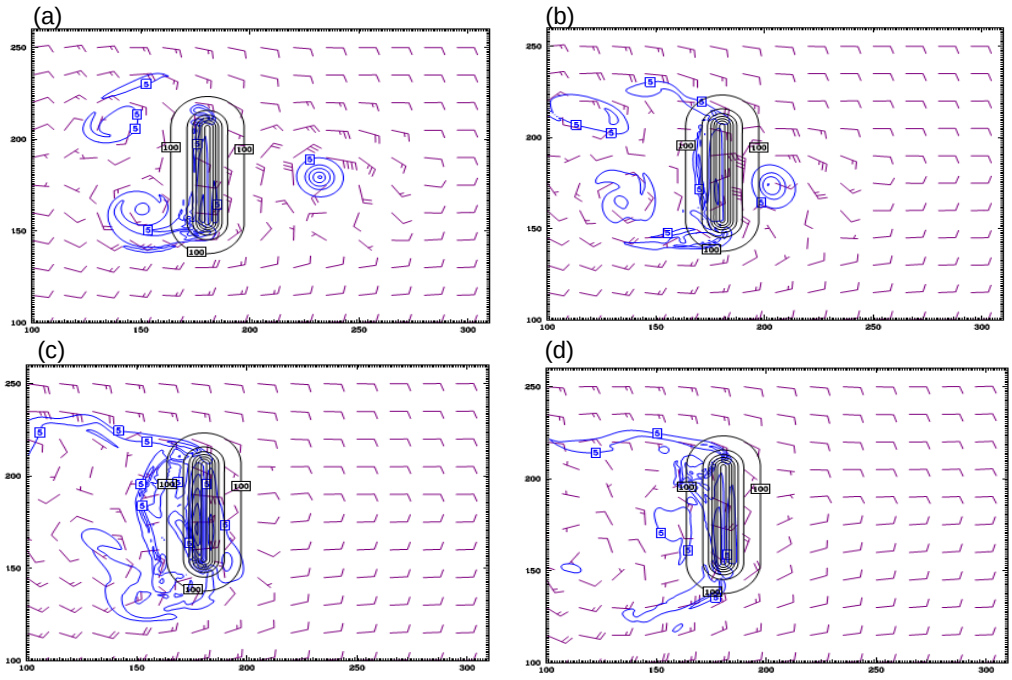

Fig. 4.2: [M2NHNP] The 900-hPa relative vorticity ($1x10^{-5}$ s^{-1}) and wind vectors simulated by a dry flow (no latent heating & no PBL) with a bogus vortex over a 2-km high mountain at (a) 72 h, (b) 108 h, (c) 144 h, and (d) 180 h.